CATALYTIC EFFECTS IN THE ELECTROCHEMICAL REACTIONS INVOLVING NICKEL AND CYSTEINE. VOLTAMMETRIC STUDIES

Florinel Gabriel BĂNICĂ and Elena DIACU

Polytechnic Institute of Bucharest,
Faculty of Industrial Chemistry, Spl. Independenței 313, Bucharest, Romania

Received April 27, 1990
Accepted June 5, 1990

Dedicated to the memory of Prof. J. Heyrovský on the occasion of his centenary.

The electrode reactions in the nickel–cysteine system at pH-values around 7 were studied by cyclic voltammetry on the hanging mercury drop electrode. The following processes are induced by cysteine: *1*) the catalytic reduction of the nickel ion; *2*) the anodic dissolution of the nickel amalgam by a catalytic mechanism; *3*) the catalytic evolution of hydrogen. Some analogies with the behaviour of the nickel center in hydrogenase are suggested.

Earlier polarographic investigations in the Ni^{2+}–cysteine system in ammonia buffer were mainly focused on the catalytic hydrogen evolution[1]. Detailed studies revealed some correlations between the coordination state of Ni^{2+} and the catalytic activity (ref.[2] and references therein). A catalytic nickel prewave also occurs in this system, the electrode process being strongly influenced by the adsorption of the catalyst[3].

A new impetus to the studies in this field was given by the discovery of the catalytic properties of selenocysteine. Although this compound is not able to produce the catalytic wave of the Brdička-type, it gives catalytic waves of cobalt[4] or nickel[5]. Additionally, in slightly acidic media, selenocysteine produces a catalytic hydrogen prewave (CHP) (refs[6,7]) which differs in many respects from the Brdička-type wave. Further studies[8,9] showed that cysteine itself may give such a catalytic wave. The optimum pH range is centered arround 6·5 (ref.[10]). Related compounds (cysteinyl-dipeptides[11], cysteine–ethyl ester[12]) also produce the CHP, provided both the thio- and amino- groups are available for coordination. A slow proton-transfer step was evidenced by the deuterium-isotope effect[13].

This paper presents the results of a voltammetric investigation on the electrochemical reactions involving cysteine and nickel, either in the reduced or oxidised form. Preliminary results were previously communicated[14,15].

EXPERIMENTAL

Analytical grade reagents were used through this work. The supporting electrolyte consisted of 0·024M Na_2HPO_4 and 0·024M CH_3COONa, the pH being adjusted by perchloric acid[10].

The laboratory-built hanging mercury drop electrode is a version of the Novotný-type device[16]. The drop area (computed from the height of the cadmium peak) was 2·6 mm^2. The three-electrode cell had a mercury pool as auxilliary- and a SCE as reference electrode. Pure argon was used to expell the dissolved oxygen. The curves were recorded by means of the OH 105 polarograph (Radelkis, Hungary) at a scan rate of 4 V/min (if not otherwise stated).

A typical run proceeds as follows: *1*) The mercury drop is formed by the stepwise mercury flow through the capillary during 20 s, with the electrode not connected to the polarograph. *2*) After 10 s the electrode is polarised at the initial potential (usually, −0·5 V). *3*) The record is started after additional 10 s. Deviations from this program may give erratic results.

RESULTS AND DISCUSSION

Electrochemical Reactions in the Nickel–Cysteine System

The effects of cysteine are presented in Fig. 1. In the absence of this compound, only the cathodic (−1·1 V) and anodic (0 V) nickel peaks appear, the electrode process being strongly irreversible (curve 1). Traces of cysteine split the anodic peak (curve 2). As the cysteine concentration increases, the anodic peak also increases and shifts towards more negative potentials (curves 3, 4). The formation of mercurous cysteinate induces the small shoulder on the anodic branch of the curve 4 at about −0·4 V.

In the cathodic range, cysteine induces the peak located at about −0·7 V, due to the catalytic nickel reduction. As in DC polarography[9], at higher cysteine concentrations (curve 4) another signal appears at −0·9 V. This peak, observed only under extreme conditions, is no further considered.

Finally, at potentials more negative than that of the normal nickel peak, a peculiar pattern appears on the curve 4. The location of this pattern reveals its analogy with the CHP recorded by DC polarography[9].

Each electrode process is further presented in detail.

The Catalytic Reduction of Nickel

The almost symmetrical shape of the catalytic nickel peak (Fig. 1) suggests the adsorption of the catalyst, the coverage being strongly dependent on the potential, in accord to the DC polarographic data[9,17]. The effect of cysteine concentration on the peak current is shown in Fig. 2 (curve 1). At cysteine concentrations $> 10^{-4}$ mol . $. l^{-1}$, the catalytic peak is higher than the normal nickel peak recorded in the absence of cysteine. Evidently the catalytic process has a higher rate as compared to the diffusion controlled reduction. The peak potential is also influenced by the cysteine concentration (Fig. 2, curve 2).

The peak current linearly correlates with the logarithm of the nickel ion concentration (Fig. 3). This dependence differs from that characteristic for diffusion-controlled processes. The peak potential slightly shifts towards less negative potentials as the nickel concentration increases.

As in the case of the DC polarographic nickel prewave[9], the peak current is strongly influenced by pH (Fig. 4, curve 1). This parameter also influences the peak potential (curve 2 in Fig. 4).

The peak current is a linear function on $v^{1/2}$ (v scan rate), as shown in Table I. However, the intercept of the lines differs from zero.

The catalytic nickel peak is enhanced by the previous adsorptive accumulation of cysteine. The preconcentration of cysteine as mercurous cysteinate (formed at $-0{\cdot}1$ V) is more efficient, especially in the presence of traces of copper(II).

The above observations enable to formulate the following mechanism of the catalytic reduction of nickel ion on the hanging mercury drop electrode. H_2L is $HSCH_2CH(NH_3)^+COO^-$.

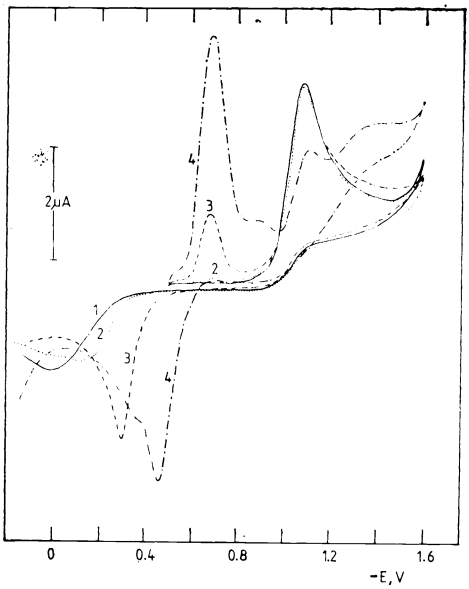

FIG. 1

Cyclic voltammograms recorded at various cysteine concentrations. pH 6·5; $2 \cdot 10^{-4}$M-Ni^{2+}. [Cysteine], mol l^{-1}: 1 0; 2 $5 \cdot 10^{-7}$; 3 $5 \cdot 10^{-6}$; 4 $5 \cdot 10^{-5}$

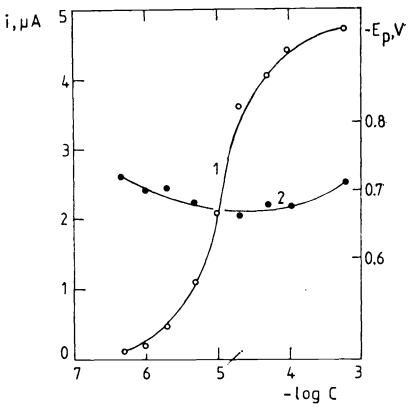

FIG. 2

Effect of cysteine concentration (in mol l^{-1}) on the catalytic nickel peak. pH 6·5; $2 \cdot 10^{-4}$M-Ni^{2+}; 1 peak current; 2 peak potential

$$(H_2L)_{sol} \xrightarrow{\text{diff.}} (H_2L)_{ads} \qquad (1)$$

$$(H_2L)_{ads} \rightleftarrows (L^{2-})_{ads} + 2\,H^+ \qquad (2)$$

$$(L^{2-})_{ads} + Ni^{2+} \rightleftarrows [NiL]_{ads} \qquad (3)$$

$$[NiL]_{ads} + 2\,e \rightarrow Ni(0) + (L^{2-})_{ads} \qquad (4)$$

TABLE I

The parameters of the straight lines $i_{p,c} = a + bv^{1/2}$ ($i_{p,c}$ is the catalytic peak current in μA; v ranges between 0·5 and 4 V/min). pH 6·5; $2 \cdot 10^{-4}$ M-Ni^{2+}

[Cysteine], mol l^{-1}	$5 \cdot 10^{-6}$	$2 \cdot 10^{-5}$	$1 \cdot 10^{-4}$
a	0·17 ± 0·03	0·11 ± 0·06	−0·36 ± 0·09
b	0·45 ± 0·02	1·65 ± 0·05	2·50 ± 0·07
Correlation coefficient	0·997	0·999	0·999

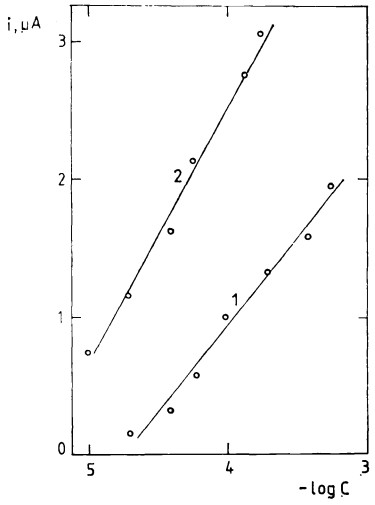

FIG. 3

Influence of nickel concentration (in mol l^{-1}) on the height of the catalytic nickel peak. pH 6·5; [cysteine], mol l^{-1}: 1 $5 \cdot 10^{-6}$; 2 $1 \cdot 10^{-4}$

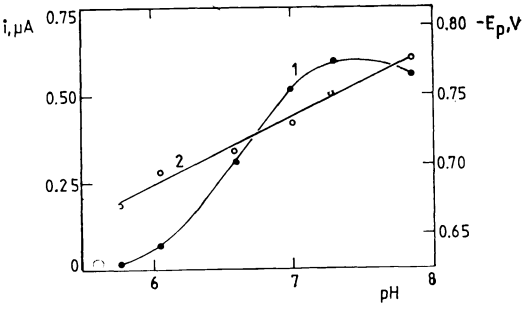

FIG. 4

Effect of pH on the height (1) and on the potential (2) of the catalytic nickel peak. [Cysteine] = $2 \cdot 10^{-6}$ mol l^{-1}; [Ni^{2+}] = $2 \cdot 10^{-4}$ mol l^{-1}

The step (*1*) gives the peculiar dependence of the peak current on the cysteine concentration (Fig. 2) since the rate of the catalyst accumulation in the adsorbed state increases at higher concentrations. The influence of the scan rate (Table I) is also due to the adsorption. Indeed, lower values of the scan rate permit the accumulation of higher amounts of adsorbed catalyst, but, simultaneously, produce a more advanced depletion of the nickel ion near the electrode before the attainment of the peak potential.

The pH influences the reaction rate by means of the step (*2*), formulated as above since at pH < 8 cysteine is protonated[18]. As concerns the combining ratio of the reducible complex, it is supported by the analogy with the nickel–cysteinyl–dipeptide system, where the value 1 was firmly established[17]. According to the well known rules[19], the high asymmetry of the coordination sphere induced by the first ligand-molecule enhances the electron-transfer rate constant. Consequently, the very fast reduction hinders the formation of higher nickel–catalyst complexes.

The catalytic nickel peak proves to be suitable for sensitive determination of cysteine by cathodic stripping voltammetry. As compared to the procedure using the cathodic peak of mercurous cysteinate, the catalytic peak is not obscured by simple thiols. The preconcentration in the presence of copper ions (according to ref.[20]) improves the sensitivity.

The Anodic Dissolution of Nickel in the Presence of Cysteine

As shown in Fig. 1, traces of cysteine influence the dissolution of nickel, both the current and the potential of the anodic peak being strongly modified. The product of the anodic reaction is the nickel ion, as demonstrates the correlation between the anodic scan reversal potential and the height of the nickel peak recorded during the second cathodic scan.

The current of the anodic peak is enhanced by the previous deposition of nickel at constant potential. However, the deposition potential influences only the peak current but not its potential.

A charge-balance was performed by stopping the potential scan at the value corresponding to the maximum anodic current (−0·1 V in the absence and −0·30 V in the presence of cysteine). The decay of the anodic current at constant potential was further recorded. The amount of electricity transferred during the nickel ion reduction (Q_c) or the anodic oxidation (Q_a) were evaluated by the planimetry of the areas limited by the curves recorded during the cathodic (respectively anodic) scan. The cysteine concentration was so low ($2 \cdot 10^{-6}$ mol l^{-1}) that the charge transferred during the formation of mercurous cysteinate can be neglected. The correction for the residual current was performed using a cyclic voltammogram recorded in the supporting electrolyte alone. The results are presented in Table II. According to these data, in the presence of cysteine both Q_c and Q_a are enhanced due to the

catalytic reduction. Both in the presence or in the absence of cysteine Q_c is higher than Q_a, denoting the partial inactivation of the nickel amalgam. However, the ratio Q_a/Q_c is not influenced by cysteine. Consequently cysteine influences only the mechanism of the anodic reaction of nickel but not the properties of the amalgam nor the reactivity of the various forms of nickel dispersed in the mercury electrode.

Both the current and the potential of the anodic peak vary linearly with the logarithm of cysteine concentration in a large region (Fig. 5), but its level becomes comparable to that of the nickel ion.

The concentration of nickel ion does not influence the potential of the anodic peak but modifies the peak current according to the following equation (at pH 6·50 and $5 . 10^{-6}$M cysteine):

$$i_p = 5{\cdot}93 + 1{\cdot}16 \log C_{Ni^{2+}} , \qquad (5)$$

where i_p is in μA and $C_{Ni^{2+}}$ in mol l^{-1}. At higher cysteine concentrations the peak current cannot be rigorously evaluated due to the formation of mercurous cysteinate.

The effects of pH on the anodic peak are shown in Table III. The peak current reaches maximum at pH about 6 and decreases as pH shifts towards lower or higher values. The peak potential becomes more negative with the increase of pH. The peak

TABLE II

Coulometric data for the reduction (Q_c) and the oxidation (Q_a) of nickel. pH 6·5; $2 . 10^{-4}$M-Ni^{2+}

[Cysteine], mol l^{-1}	Q_c, C	Q_a, C	Q_a/Q_c
0	$3{\cdot}89 . 10^{-5}$	$1{\cdot}04 . 10^{-5}$	0·263
$2 . 10^{-6}$	$4{\cdot}33 . 10^{-5}$	$1{\cdot}15 . 10^{-5}$	0·265

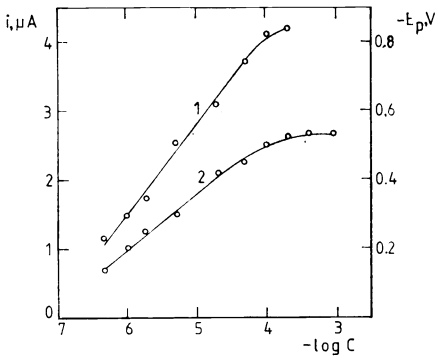

FIG. 5

Influence of cysteine concentration (in mol . l^{-1}) on the height (1) and on the potential (2) of the anodic peak of nickel. pH 6·5; $[Ni^{2+}] = 2 . 10^{-4}$ mol l^{-1}

width (expressed by $E_p - E_{p/2}$, where E_p is the peak potential and $E_{p/2}$ the halfpeak potential) also varies with pH. Under the same conditions the parameters of the anodic peak recorded in the absence of cysteine are not dependent on pH (i_p = = 1·03 ± 0·12 μA; E_p = −0·01 ± 0·01 V; $E_{p/2}$ = −0·17 ± 0·01 V for pH ranging between 2·2 and 7·5). Additionally, at pH < 6 the catalytic cathodic peak disappears and the diffusion-controlled reduction remains the only way to produce zerovalent nickel. This change, however, does not introduce irregularities in the anodic current –pH dependence. It is also important to note that the decrease of pH influences the anodic peak in the same way as the decrease of cysteine concentration at constant pH (Fig. 2).

In conclusion, the intensity of the anodic process depends on both the cysteine concentration and its protonation degree. The effect of cysteine appears at much lower concentrations as compared to that of the nickel ion, proving the catalytic character of the electrode process. It must be stated that in the potential range of the anodic peak cysteine is strongly adsorbed[9], especially at higher pH values. Taking into account these remarks, the anodic dissolution of nickel in the presence of cysteine may be represented by the following mechanism, where HL^- is $HSCH_2CH.NH_2COO^-$:

$$Ni(0) + m(HL^-)_{ads} \rightleftarrows [Ni(0)(HL^-)_m]_{ads}, \quad (6)$$

$$[Ni(0)(HL^-)_m]_{ads} \rightarrow [Ni(II)(HL^-)_m]_{ads} + 2e, \quad (7)$$

$$[Ni(II)(HL^-)_m]_{ads} + kH_2O \rightleftarrows [Ni(H_2O)_k]^{2+} + m(HL^-)_{ads}. \quad (8)$$

The formation of a zerovalent nickel complex in the step (6) is favoured by the back-donation effect[21] and the participation of such compounds in the catalytic hydrogen evolution is widely accepted[22]. The higher rate constant of the electron transfer involving the zerovalent complex as compared to free Ni(0) may be connected with the strong polarization induced by complexation. The aquation of the product of the step (7) permits the diffusion of the nickel ion into the bulk of the solution.

TABLE III

The influence of pH on the anodic peak of nickel. 5 . 10^{-6}M Cysteine, 2 . 10^{-4}M-Ni^{2+}

pH	7·50	6·50	5·80	5·00	4·20	3·20	2·25
$-E_p$, V	0·32	0·31	0·29	0·26	0·18	0·12	0·075
$-(E_p - E_{p/2})$, V	0·07	0·05	0·04	0·035	0·045	0·055	0·085
$i_{p,a}$, μA	1·80	2·00	2·20	2·06	1·66	1·42	1·28

The anodic reaction is not dependent on the deposition potential or the mechanism of Ni^{2+} reduction. Besides, only two types of anodic reactions are observed in this system, namely the normal one (in the absence of cysteine) and the catalytic process. Both reactions involve the same kind of active nickel representing only a fraction of the total amount of metal formed during the cathodic scan. The coulometric data show that a part of the supersaturated nickel amalgam becomes inactive to the oxidation. This is due to the slow formation of an intermetallic compound, formulated as $NiHg_3$ in ref.[23] or $NiHg_4$ in ref.[24]. However, the composition of the solution, as well as the mechanism of Ni amalgam formation do not influence the properties and the behaviour of Ni(0).

Anodic effects of this kind were first observed in the presence of chloride[25] and were explained by a catalytic mechanism[23,26]. In contrast to cysteine, the effect of Cl^- is observed at very high concentrations. This difference cannot be assigned only to the higher surface activity of cysteine. The higher ability of thiol to stabilize low oxidation states may be more important.

It is interesting to compare the anodic reactions of nickel and cobalt amalgams. In the presence of cysteine[27] or thioglycollic acid[28] the cobalt amalgam gives several anodic peaks. In contrast to nickel, the anodic behaviour of cobalt depends on the mechanism of the generating cathodic process, which may be either of the catalytic type or diffusion-controlled. Cobalt deposition in the presence of bovine serum albumin also gives various forms of Co(0) (ref.[29]). In conclusion, the behaviour of cobalt is more involved, probably due to its lower solubility in mercury as compared to nickel.

The Catalytic Hydrogen Evolution

During the cathodic scan cysteine induces not only the catalytic hydrogen evolution, but also the reduction of nickel ion in the range of the catalytic peak. This is why the voltammogram recorded in the absence of cysteine (Fig. 6, curve 1) cannot be used as the base-line for the catalytic hydrogen current observed on the first (cathodic) scan (Fig. 6, curve 2). Conversely, the reverse scan produces a curve which is practically not influenced by the catalytic nickel reduction due to the advanced Ni^{2+} depletion. Accordingly, through this work, the catalytic hydrogen current (i_1) was measured on the reverse side of the cyclic voltammogram, as shown in Fig. 6.

It was demonstrated[15] that the catalytic hydrogen evolution on the static mercury electrode produces a pattern characteristic for a steady-state process. In other words, this pattern is correctly described by the equation of the irreversible polarographic wave and the catalytic hydrogen current, as defined in Fig. 6, is a true limiting current. The corresponding voltammetric pattern is further termed as the catalytic hydrogen step (CHS). The half-height potential of the CHS ($-1{\cdot}22$ V) is in a fair accord with the half-wave potential of the CHP recorded by DC polarography[8,9]

According to refs[30,31] this kind of voltammetric pattern is produced by the catalytic electrode processes provided the following condition is fulfilled:

$$(RT/\alpha nFv)\, k'C^* > 1 \; ; \qquad (9)$$

R, T, α, n and F have usual meanings, k' is the rate-constant of the parallel chemical reaction which regenerates the reducible species and C^* is the bulk concentration of the non-reducible species involved in this reaction. For the process considered here the catalyst is the low-valency nickel complex formed by the reduction of the cysteinate complex and the parallel chemical reaction consists in the protonation of the former[6,9]. C^* is the concentration of the proton donor i.e. the acid component of the buffer-system. The above inequality (9) permits to evaluate the lower limit of k' as about 100 $mol^{-1}\, l\, s^{-1}$ but this constant may, in fact, be much higher.

In contrast to the mechanism considered in refs[30,31] in this system the catalyst is not a stable species but an unstable intermediate produced during the nickel reduction. The gradual depletion of Ni^{2+} during the record explains the hysteresis of the cyclic voltammogram in the range of the CHS (Fig. 6). This behaviour differs from that of a process catalysed by a stable species present in the bulk of the solution. In the last case, no hysteresis appears if the relation (9) is fulfilled.

The Ni^{2+} exhaustion also produces the variation of i_l with the scan rate, at variance with the theoretical results of refs[30,31].

Several experiments were performed in order to assess the effects of nickel coordination by cysteine. Thus, the cysteine concentration near the electrode surface

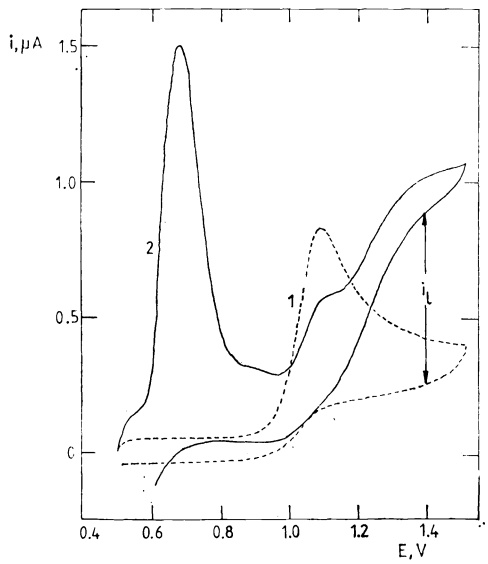

FIG. 6

Cyclic voltammograms recorded in the range of the catalytic hydrogen evolution. pH 6·5; $1 \cdot 10^{-4}$M-Ni^{2+}. [Cysteine], mol l^{-1}: 1 0; 2 $1 \cdot 10^{-4}$

can be enhanced by the previous accumulation at 0 V. In the presence of 10^{-6}M cysteine, after 5 min of accumulation in the stirred solution, the CHS is clearly developed on the cathodic branch of the voltammogram, but not on the reverse one. In the same solution, the CHS does not form if the record is not preceded by the accumulation. It is thus clearly demonstrated that cysteine is not adsorbed in the range of the CHS and the above effect is due to the molecules present in the reaction layer. This layer is, however, readily depleted of cysteine and, consequently, the catalytic effect is absent during the reverse scan.

The bulk concentration of cysteine also influences the catalytic hydrogen current (Fig. 7). The shape of the curve in Fig. 7 is due to the adsorption of cysteine during the steps preceeding the start of the record. This process, which enhances the cysteine concentration in the reaction layer at the potentials of the CHS, is very slow at low bulk concentrations.

The effect of the nickel ion concentration on i_1 is shown in Fig. 8 (curve 1).Curve 2 in the same figure represents the nickel reduction current in the absence of cysteine, measured on the reverse scan, at the same potential as i_1. The correlation of the

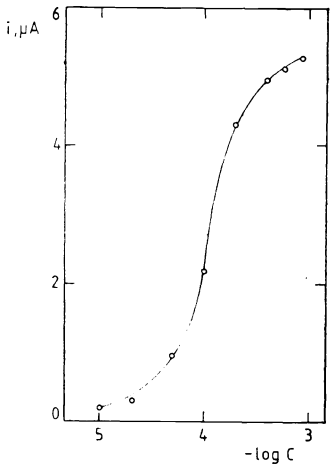

FIG. 7

Effect of cysteine concentration (in mol l^{-1}) on the catalytic hydrogen current. pH 6·5; $2 \cdot 10^{-4}$M-Ni^{2+}

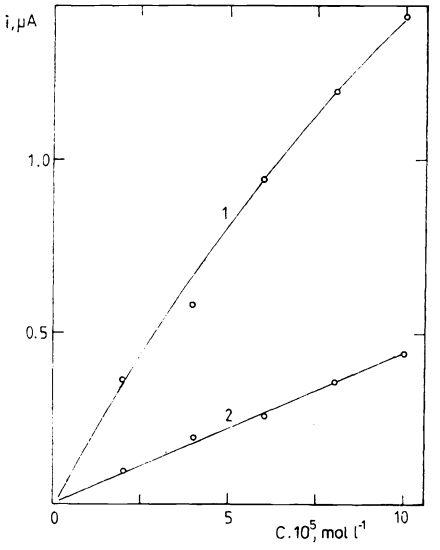

FIG. 8

Effect of nickel ion concentration on the catalytic hydrogen current (1) and on the Ni^{2+} reduction current recorded in the absence of cysteine (2). pH 6·5; $1 \cdot 10^{-4}$M cysteine

catalytic hydrogen current with the nickel ion concentration near the electrode is obvious.

Nickel deposition prior to the record of the CHS diminishes the catalytic hydrogen current. Thus, the possibility of heterogeneous catalysis by nickel clusters is excluded. The absence of an anodic process assignable to the hydrogen oxidation also points to the absence of any role played by metallic nickel.

The above data confirm the reaction mechanism previously formulated[6,9]. As a particular feature, under the voltammetric conditions the parallel chemical reaction represents the rate-determining step, at least at low scan rates. As shown by the deuterium isotope effect[13], this step is a proton-transfer reaction. By contrast, DC polarography evidences only a partial kinetic character of the limiting catalytic hydrogen current[9] the rate of the electrode process being also influenced by diffusion.

The catalytic hydrogen reduction on the hanging mercury electrode is not dependent on the concentration or the state of nickel amalgam. Only the parameters influencing the formation of nickel–cysteine complexes are important. The voltammetric data also support the homogeneous character of the parallel proton-transfer step.

CONCLUSIONS

Cysteine strongly influences both the reduction of nickel ion and the anodic dissolution of the nickel amalgam. These processes involve the interaction of adsorbed cysteine with the reacting nickel species. However, the mechanisms are different and these reactions do not represent the two directions of evolution of a reversible process. The anodic effect demonstrates the capacity of cysteine to stabilise low-valency nickel species.

A low-valency, unstable, nickel complex also forms by the reduction of the Ni(II)–cysteine complex. This species catalyses the reduction of hydrogen ion, producing the CHS. A steady concentration of this intermediate is established and the rate-determining protonation step gives the CHS its peculiar shape. No evidence exists on the identity of the low-valency nickel complex involved in the anodic dissolution of nickel and that producing the catalytic hydrogen evolution.

The catalytic hydrogen evolution at circumneutral pH-values in the presence of cysteine and nickel ion evokes, in some respects, the reduction of the hydrogen ion catalysed by hydrogenase. The most striking ressemblance is the presence of sulfur-coordinated nickel centers in the structure of some varieties of this enzyme[32]. Various oxidation states of nickel in hydrogenase were detected[33]. Although the coordination of nickel by cysteine residues in hydrogenase is to be supposed, the macromolecular structure surely induces some differences as compared to the simple nickel–cysteine complexes. However, it seems to be useful to pay more attention to the processes of the CHP-type as models for the hydrogenase-catalysed reactions.

REFERENCES

1. Căluşaru A.: J. Electroanal. Chem. Interfacial Electrochem. *15*, 269 (1967).
2. Kuik M.: Collect. Czech. Chem. Commun. *36*, 1009 (1971).
3. Kůta J.: Z. Anal. Chem. *216*, 243 (1966).
4. Căluşaru A., Voicu V.: J. Electroanal. Chem. Interfacial Electrochem. *20*, 463 (1969).
5. Căluşaru A., Voicu V.: J. Electroanal. Chem. Interfacial Electrochem. *32*, 427 (1971).
6. Căluşaru A., Voicu V.: Experientia *29*, 140 (1973).
7. Căluşaru A., Voicu V.: J. Electroanal. Chem. Interfacial Electrochem. *43*, 257 (1973).
8. Căluşaru A., Bănică F. G.: J. Electroanal. Chem. Interfacial Electrochem. *47*, 190, 554 (1973).
9. Bănică F. G., Căluşaru A.: J. Electroanal. Chem. Interfacial Electrochem. *145*, 389 (1983).
10. Bănică F. G., Diacu E.: Rev. Roum. Chim. *35*, 9 (1990).
11. Bănică F. G.: J. Electroanal. Chem. Interfacial Electrochem. *171*, 351 (1984).
12. Bănică F. G., Florea M., Moraru M.: J. Electroanal. Chem. Interfacial Electrochem. *285*, 281 (1990).
13. Bănică F. G., Căluşaru A.: J. Electroanal. Chem. Interfacial Electrochim. *158*, 47 (1983).
14. Diacu E., Bănică F. G.: Bull. Soc. Chim. Belg. *96*, 251 (1987).
15. Bănică F. G., Diacu E., Luca C.: Bull. Soc. Chim. Belg. *96*, 485 (1987).
16. Novotný L.: *Proceedings of the J. Heyrovský Memorial Congress on Polarography, Prague 1980*; Vol. II, p. 129.
17. Bănică F. G.: Talanta *32*, 1145 (1985).
18. Benesch R. E., Benesch R.: J. Am. Chem. Soc. *77*, 5877 (1955).
19. Heyrovský J., Kůta J.: *Principles of Polarography*, p. 226. Publishing House of the Czechoslovak Academy of Sciences, Prague 1965.
20. Forsman U.: J. Electroanal. Chem. Interfacial Electrochem. *152*, 214 (1983).
21. Malatesta L., Cenini S.: *Zerovalent Compounds of Metals*. Academic Press, New York 1974.
22. Căluşaru A.: *Electrodeposition of Metal Powders*, p. 207. Elsevier, Amsterdam 1979.
23. Žutić V., Batel R., Chevalet J.: J. Electroanal. Chem. Interfacial Electrochem. *105*, 115 (1975).
24. Kozin L. F., Nigmetova P. S., Dergatcheva M. B.: *Termodinamika Binarnykh Amalgamnykh Sistem*, p. 282. Nauka, Alma-Ata 1977.
25. Kemula W., Jeftič L., Galus Z.: J. Electroanal. Chem. Interfacial Electrochem. *10*, 387 (1965).
26. Chevalet J., Žutić V.: J. Electroanal. Chem. Interfacial Electrochem. *44*, 411 (1973).
27. Anzenbacher P., Kalous V.: Collect. Czech. Chem. Commun. *44*, 2418 (1979).
28. Anzenbacher P., Kalous V.: Colect. Czech. Chem. Commun. *38*, 3362 (1973).
29. Kihara S., Matsui M., Yoshida Z.: J. Electroanal. Chem. Interfacial Electrochem. *197*, 331 (1986).
30. Savéant I. M., Vianello E.: Electrochim. Acta *8*, 905 (1963); *10*, 905 (1965); *12*, 629 (1967).
31. Nicholson R. S., Shain I.: Anal. Chem. *36*, 706 (1964).
32. Eidsness M., Sullivan R. J., Cramer S. P., Scott R. A. in: *Bioinorganic Chemistry of Nickel* (J. R. Lancaster, Ed.), Chap. 5. VCH Publishers, Deerfeld Beach 1987.
33. Okura I.: Coord. Chem. Rev. *68*, 53 (1985).

Translation revised by K. Micka.